Current Microbiology (2023) 80:47
https://doi.org/10.1007/s00284-022-03108-9

# A Comprehensive in vitro and in silico Assessment on Inhibition of CYP51B and Ergosterol Biosynthesis by Eugenol in *Rhizopus oryzae*

**Jignesh Prajapati[1] · Priyashi Rao[1] · Lipi Poojara[1] · Dhaval Acharya[2] · Saumya K. Patel[3] · Dweipayan Goswami[4] · Rakesh M. Rawal[1,5]**

Received: 2 April 2022 / Accepted: 3 November 2022 / Published online: 20 December 2022


## Abstract

Mucormycosis, also known as Zygomycosis, is a disease caused by invasive fungi, predominantly *Rhizopus* species belonging to the Order of *Mucorales*. Seeing from the chemistry perspective, heterocyclic compounds with an "azole" moiety are widely employed as antifungal agent for minimising the effect of mucormycosis as a prescribed treatment. These azoles serve as non-competitive inhibitors of fungal CYP51B by predominantly binding to its heme moiety, rendering its inhibition. However, long-term usage and abuse of azoles as antifungal medicines has resulted in drug resistance among certain fungal pathogens. Hence, there is an unmet need to find alternative therapeutic compounds. In present study, we used various in vitro tests to investigate the antifungal activity of eugenol against *R. oryzae/R. arrhizus*, including ergosterol quantification to test inhibition of ergosterol production mediated antifungal action. The minimum inhibitory concentration (MIC) value obtained for eugenol was 512 µg/ml with reduced ergosterol concentration of $77.11 \pm 3.25\%$ at MIC/2 concentration. Further, the molecular interactions of eugenol with fungal CYP51B were meticulously studied making use of proteomics in silico study including molecular docking and molecular dynamics simulations that showed eugenol to be strongly interacting with heme in an identical fashion to that shown by azole drugs (in this case, clotrimazole was evaluated). This is the first of a kind study showing the simulation study of eugenol with CYP51B of fungi. This inhibition results in ergosterol synthesis and is also studied and compared with keeping clotrimazole as a reference.

✉ Dweipayan Goswami
dweipayan.goswami@gujaratuniversity.ac.in

✉ Rakesh M. Rawal
rakeshrawal@gujaratuniversity.ac.in;
rakeshmrawal@gmail.com

[1] Department of Biochemistry and Forensic Science, University School of Sciences, Gujarat University, Ahmedabad, Gujarat 380009, India

[2] Department of Microbiology, B N Patel Institute of Paramedical and Sciences, Anand, Gujarat 388001, India

[3] Department of Botany, Bioinformatics and Climate Change Impacts Management, School of Sciences, Gujarat University, Ahmedabad, Gujarat, India

[4] Department of Microbiology and Biotechnology, University School of Sciences, Gujarat University, Ahmedabad, Gujarat 380009, India

[5] Department of Life Science, University School of Sciences, Gujarat University, Ahmedabad, Gujarat 380009, India

**Graphical Abstract**

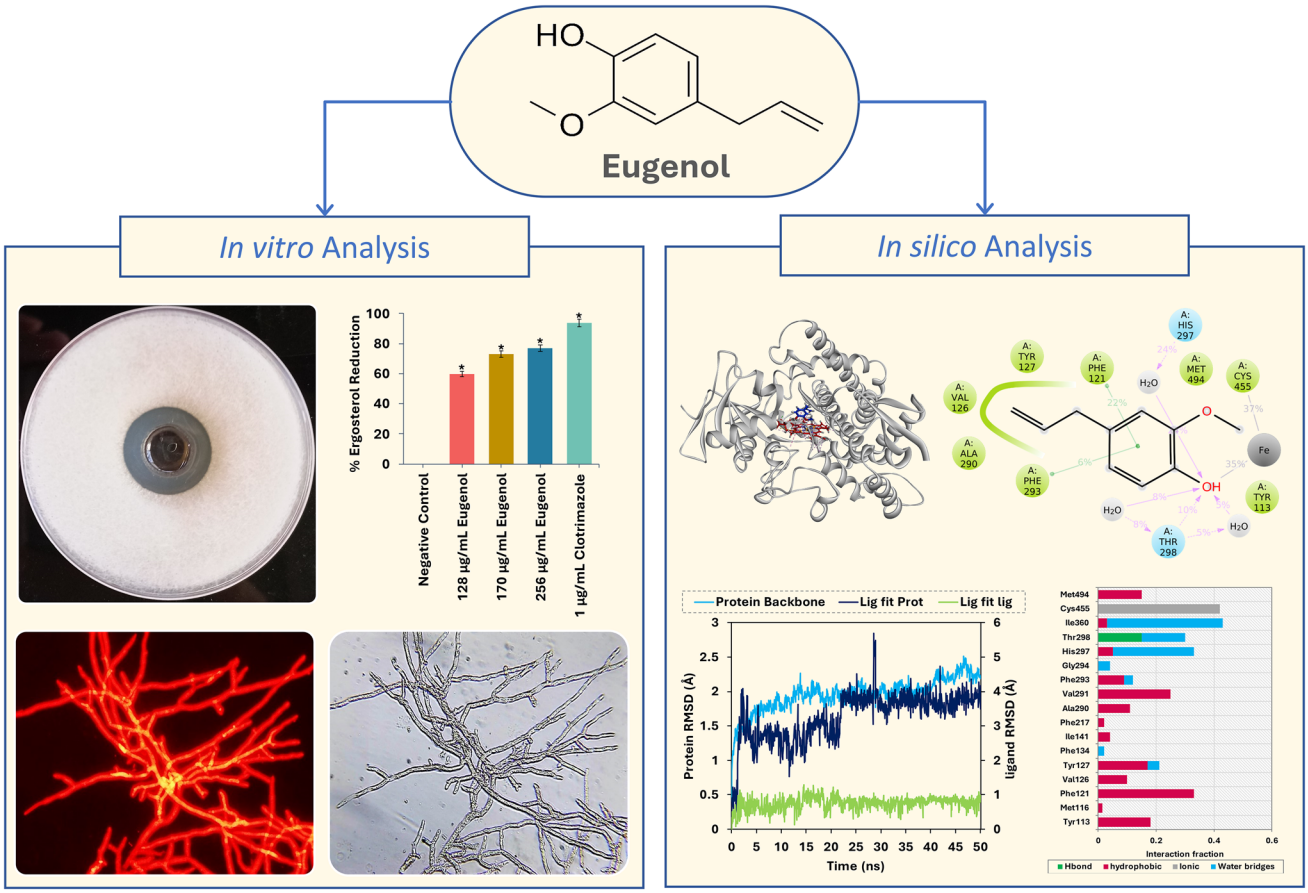


## Introduction

Mucormycosis, also known as Zygomycosis previously, is an invasive form of fungal infection primarily caused by *Rhizopus* species belonging to the order of *Mucorales* [1]. With the upsurge in incidence of infectious diseases, the global prevalence of mucormycosis has increased in the recent decade. This lethal pathogen commonly targets immunocompromised patients enduring conditions like ketoacidosis related to diabetes mellitus, neutropenia, organ-transplantation having increased serum iron levels and administering high-dose corticosteroids [2]. In recent times, the pandemic of SARS-CoV-2 infection has paved the way for comorbidities associated with secondary infections post Coronavirus disease 2019 (COVID-19). Often, the use of steroids that appear to help in prevention of cytokine storm during COVID-19 infection leads to a weakening of the body's immune system while overdriving to fight the viral infection [3]. Majority of the rhino-orbital-cerebral mucormycosis (ROCM) infection is initiated by the inhalation of spores, originated ~70% of the times from *Rhizopus oryzae* [2], hence it is notoriously known as one of the most common mucormycosis agent. *R. oryzae* spores germinate in the host to form hyphae, which then are able to invade the host to cause tissue necrosis [4].

From a class of drugs available in the market, the heterocyclic molecules possessing "azole" moiety have been widely used as an antifungal drug, and they are today the most widely applied class of antifungals in medicine. These azole agents bind to fungal CYP51's heme group, altering the catalytically active structure and functioning as non-competitive inhibitors. In several investigations, the potency of azoles as Lanosterol 14-α-Demethylase (CYP51) inhibitors is being established. Inhibition of CYP51 eventually leads to impairment of ergosterol production, evidence of which is given in the literature [5, 6]. However, long-term usage of several azoles as antifungal medicines has resulted in drug resistance among certain fungal pathogens [7–9]. Resistance to commonly prescribed medications, particularly fluconazole, has already been linked to genetic alterations [7]. As a result, "azole" research is beginning to shift toward developing new effective therapeutic compounds to overcome this key stumbling block.

Natural compounds have recently attracted a lot of attention due to their wide range of applications, including antibacterial, antifungal, anti-diabetic, anti-cancer, larvicidal, and biological activities [10–15]. Eugenol, a phenol-like aromatic phytochemical, is obtained as the major constituent of clove oil (*Syzygium aromaticum*) [16] and is also obtained from the essential oils of other plant species belonging to the Lamiaceae, Lauraceae, Myrtaceae, and Myristicaceae family [17]. Eugenol is known to have antioxidative, analgesic, antimutagenic, antiplatelet, anti-swelling, and anti-inflammatory effects. It also possesses antimicrobial properties against a variety of human pathogens, including a variety of Gram-positive and Gram-negative bacteria, fungi, and parasites [18, 19].

The targeted research strike to fill the research gap that is, the well identified anti-fungal agent eugenol, till date has not been studied for its ability to interact with fungal CYP51B, that is the crucial target for azole antifungal drugs. Briefly, CYP51B is the key enzyme performing rate limiting step in the formation of ergosterol, which is the key component (a fungal sterol) in the fungal cell wall, and any inhibition in this enzyme can lead to decrease in ergosterol content in the fungal cell eventually leading to its death. Here, we accessed eugenol for its ability to reduce ergosterol production and for its antifungal properties taking *R. oryzae/R. arrhizus* as test fungal organism. The findings of our research showed eugenol to wreck the fungal membrane *R. oryzae/R. arrhizus* by distorting ergosterol biosynthesis and validation of eugenol to interact with CYP51B was done using computational simulations.

In the present study, we used in vitro analysis to investigate the antifungal activity of eugenol against *R. oryzae/R. arrhizus*, including ergosterol quantification to test inhibition of ergosterol production mediated antifungal action. To confirm our in vitro findings, we performed molecular docking and molecular dynamics (MD) simulation investigation of eugenol with Lanosterol 14-α-Demethylase of *R. oryzae/R. arrhizus* (CYP51B). To the best of our knowledge, the possibility of eugenol interacting with CYP51B was investigated for the first time with promising validated results.

## Materials and Method

Eugenol was purchased from HiMedia, India and diluted in DMSO (dimethyl sulfoxide) to prepare a stock solution, and then sterile distilled water was used to make 2048 µg/ml solution, which was then used to investigate antifungal activity.

### Isolation and Identification of Fungal Pathogen

Isolation of a fungal pathogen was carried out at the central facility lab, School of Sciences, Gujarat University. Left over Infected tissue sample of mucormycosis patient was donated by Speciality Microtech Lab, Navrangpura, Ahmedabad. A tissue sample was divided into several parts aseptically and inoculated onto potato dextrose agar (PDA) as a culture medium. The plates were then incubated for 48 to 72 h at 28 °C. Isolated fungus was grown again on fresh PDA medium and looked at using traditional mycological methods, such as morphological and microscopic traits of pure culture. The most important characteristics to identify fungi morphologically are the spores (shape and size), and fruiting bodies and to some extent mycelia. Isolated fungus was sub-cultured on fresh PDA medium and observed on daily basis. Microscopic examination was performed using Lactophenol cotton blue stanning.

Furthermore, isolated fungus was identified through molecular identification method. The DNA was extracted from a two-day-old culture using a previously described protocol [20]. The fungus's internal transcribed spacers (ITS) region was amplified using polymerase chain reaction (PCR) with the universal ITS primers ITS4 (5′ TCCTCCGCTTAT TGATATGC3′) and ITS5 (5′ GGAAGTAAGTCGTAACAA 3′) and sequenced using the 96-capillary ABI 3730xl Genetic Analyzer (Applied Biosystems™). Once the sequence was obtained, the BLASTn search tool (http://www.ncbi.nlm.nih.gov) was used to examine nucleotide sequence homology. The genus and species were determined using the highest percent similarity of identical sequences already available in the database. The obtained sequence was deposited in GenBank, and an accession number was assigned. Furthermore, the 18S rRNA sequences of the type species belonging to *Rhizopus* were downloaded and aligned along with the obtained sequence of isolated fungus by ClustalW using MEGA 11.0 software [21] and Neighbour-Joining phylogenetic tree was constructed with the bootstrap value of 1000 replications.

### In Vitro Assays

To investigate the antifungal activity of eugenol against *R. oryzae/R. arrhizus* in several in vitro tests, a sterile saline solution containing 0.9% NaCl and 0.05% Tween-20 was formulated with fungal spores. After diluting the spore solution to $1 \times 10^6$ spores per millilitre, it was employed as an inoculum in subsequent experiments.

### Antifungal Activity Using Agar Well Diffusion Method

The antifungal activity of eugenol was assessed using an agar well diffusion assay [22]. Briefly, Petri plates containing PDA were inoculated aseptically with 200 µl spore suspension through the spread plate technique. Following the inoculation of the organism, 8 mm well was made using

cork-borer and filled with 100 µl of eugenol. Sterile distilled water as a negative control and clotrimazole was employed as a positive control. All the plates were prepared in triplicate and incubated at 28 °C for 48 h. The inhibition zone dimeters were measured in millimetres (mm) and zones bigger than 1 mm were considered a positive result.

## Minimum Inhibitory Concentration (MIC)

The minimum inhibitory concentration (MIC) of eugenol and clotrimazole against *R. oryzae/R. arrhizus* was measured in accordance with CLSI reference document M38-A [26] using the microdilution broth technique for filamentous fungi. In brief, the fungal spores were cultured in RPMI-MOPS media (pH 7.2) for 18 h at 28 °C in the presence of various concentrations of eugenol (1.22 to 2048 µg/ml) and clotrimazole (1.22 to 2048 µg/ml) in two different sets of experiments. Here, clotrimazole was used as a positive control, eugenol was used as test, and media without drug was used as a negative growth control. The MIC value was determined as the lowest concentration capable of completely inhibiting fungal growth. The result was drawn from the average of three replicates.

## Ergosterol Biosynthesis Inhibition Assay

Total intracellular sterols were extracted from *R. oryzae/R. arrhizus* and measured using spectrophotometric method with minor modifications as reported in earlier publications [5, 23]. Briefly, 50 ml of PDB broth was prepared, autoclaved, and inoculated with 50 mL of $1 \times 10^6$ spores/ml. For 3 h, all flasks were then incubated at 28 °C and 120 rpm. Eugenol was then introduced to three erlenmeyer flasks at sub-MIC concentrations at MIC/2, MIC/3, and MIC/4 levels. Moreover, clotrimazole (1 µg/ml) was also considered as positive control and one untreated flask was considered as negative control. To allow the fungus to propagate, all the erlenmeyer flasks were incubated for 48 h at 28 °C and 120 rpm. After that, the mycelia were recovered by centrifugation at 3000 rpm for 15 min and rinsed once with sterile distilled water. The mycelia's net wet weight was calculated for further calculations. To extract the sterol from collected mycelia, first the mycelia were treated with the 3 mL of 25% alcoholic potassium hydroxide (KOH) and incubated at 85 °C for about one hour. Once the incubation is over, n-heptane and distilled water was added in 3:1 ratio and vortexed for three minutes. The separated n-heptane layers were then transferred into new vials, diluted five times in 100 percent ethanol, and scanned in a UV–visible spectrophotometer (LABINDIA, UV3000 + , INDIA) between 230 and 350 nm. The obtained curve with four peaks showed the presence of ergosterol and the late sterol intermediate 24(28) dehydroergosterol (DHE) in the sample. To nullify the concentration of DHE and quantify ergosterol concentration as a percentage of the wet weight of mycelia, the following equation was used:

$$\%ergosterol = \frac{F}{Mycelia\_weight}\left[\left(\frac{A_{281.5}}{290}\right) - \left(\frac{A_{230}}{518}\right)\right] \quad (1)$$

where, F is the factor for dilution in ethanol and 290 and 518 are the percent extinction coefficient ($\varepsilon_{percent}$) values in percentages per centimetre for crystalline ergosterol and 24 (28) DHE in absolute alcohol solvent [24].

## Determination of Fungal Membrane Integrity

The integrity of the membrane was verified using fluorescence microscopy [29]. In PDB containing eugenol and clotrimazole, fungal spores were let to proliferate for 24 h. Thereafter, the fungi were washed in sterile phosphate buffer saline (PBS) and stained with propidium iodide (PI) for 30 min at 4 °C in the dark. Following the staining, the mycelia were washed again in PBS to remove any residual dye and then observed in fluorescent microscope (Lawrence & Mayo) at 40X magnification equipped with a green filter.

## In-Silico Interaction of Eugenol and Fungal CYP51B

CYP51B is the essential enzyme necessary for the synthesis of ergosterol, and there is substantial evidence that inhibiting this enzyme may dramatically limit ergosterol production. In addition, clotrimazole inhibits this enzyme to promote antifungal action. Consequently, the ability of eugenol to inhibit CYP51B was investigated using molecular docking and Molecular Dynamics simulations, with clotrimazole serving as the reference inhibitor. This enabled us to determine the effectiveness of eugenol's interaction with CYP51 in relation to clotrimazole.

## Molecular Docking

Since the molecular 3D structure of *R. oryzae/R. arrhizus* CYP51B has yet to be crystallised, the modelled structure of this protein from the previous research was utilized [25]. Protein was prepared using Protein preparation wizard (PrepWizard) of Maestro. This process is divided into three parts, the first part being the pre-processing, where hydrogen was added to protein, converting selenomethionine to methionine, filling missing side chain and missing loops using prime and the second part being assignment of H-bond using PROPKA at pH 7.0 for the optimization of protein followed by minimization of protein using OPLS_2005 force field in last step. Once, the protein was prepared, a grid box was generated around the protein using Receptor Grid Generation tool of Glide in Maestro.

Subsequently, both the ligands, clotrimazole (control molecule) and eugenol (test molecule), were imported to Schrödinger Maestro in SDF format to be prepared using LigPrep module [26]. On the road to preparing ligands for docking, hydrogens were added to all ligands, bond orders were assigned, bond lengths and angles were adjusted, stereochemistry was determined, and ring conformations were determined followed by setting ionization state at pH 7.0 using Epik ionization tool. Additionally, partial charges were applied using the OPLS-2005 force-field, followed by an energy minimization process. For the docking of both the molecules, Glide's extra precision (XP) mode with default settings was used along with post docking minimization step [27]. Both docked ligands were exported and evaluated using BIOVIA Discovery Studio (DS) visualizer, to explore the hydrogen bonds and hydrophobic interactions of the functional groups of ligands with amino acids present in the binding site of the protein [28].

### MM-GBSA Assay

Molecular Mechanics Generalized Born Surface Area (MM-GBSA) was applied to calculate the end point binding free energy change using the output files of both docked complexes after docking. Using the OPLS-2005 force field in Schrödinger Maestro's Prime wizard, the binding free energy change for a complex of receptors and ligands was computed [29–32]. The MM-GBSA ΔGBind score represents the molar Gibbs free energy change in the binding of receptor and ligand molecules in solution.

### Molecular Dynamics (MD) Simulations

MD simulations for both the docked complexes CYP51B-clotrimazole and CYP51B-eugenol were run for 50 ns using the Desmond package (Schrödinger Release 2018-4) [33]. For the simulation assessments, CYP51B-clotrimazole complex was taken as reference control against which the simulation result of CYP51B-eugenol was compared with. For MD simulations the virtual simulation box was prepared into which complex was placed, and then simulation box was filled with water molecules with TIP3P model, after which the ions $Cl^-$ or $Na^+$ were placed in the simulation box for neutralization. MD simulations were performed with NPT ensemble at 300 K and 1.01 bar for 50 ns. Post MD simulations assessments were performed by assessing ligand receptor interaction profiles with respect to time, types, and nature; The root mean square deviation (RMSD) and root mean square fluctuations (RMSF) assessments of trajectories were also analysed to evaluate the stability of protein–ligand complexes during the simulations run.

### Statistical Analysis

The results were expressed in mean ± SE. Differences between the means were statistically compared using unpaired t-test. The values were considered significantly different when $p < 0.05$.

### Deposited DNA Sequence

The DNA sequence of isolated fungi was submitted in the GenBank sequence database which is maintained by National Center for Biotechnology Information (NCBI) and assigned with the NCBI accession number MZ424045.

## Results

### Identification of Fungal Pathogen

White, cottony, fluffy, growth with aerial hypha was observed on PDA plate (Fig. 1a). Upon ageing, hypha become dirty white or black which can be observed in Fig. 1b. Long, slender, coenocytic mycelia having rhizoids at the nodes was observed under 40X objective lens (Fig. 1c). Sporangiospores arise in chains that are long and have sporangia, stolon, and rhizoids. The morphology and microscopic investigation of isolated fungal culture reveal that it belongs to the *Rhizopus* genus.

As represented in the phylogenetic tree (Fig. 2), the isolated fungus GU1 was classified into the clade including *Rhizopus arrhizus* strain AUMC 14,823 and *Rhizopus oryzae* strain CBS 112.07. The isolated mucormycosis fungal agent GU1 was closely related to *R. oryzae* strain CBS 112.07 and *Rhizopus arrhizus* strain AUMC 14,823 with the ITS sequence similarity of 58% and 64%, respectively. Since *Rhizopus arrhizus* is a synonym of *Rhizopus oryzae* [34], the isolated fungus was finally identified as *Rhizopus arrhizus* and sequence data was submitted to GenBank under NCBI accession number MZ424045.

### Antifungal Activity of Eugenol

Initially, the antifungal activity of eugenol was assessed against isolated *Rhizopus oryzae* through agar well diffusion assay. In the entire study, clotrimazole was considered as control. As shown in Fig. 2a, clotrimazole and eugenol showed 29 ± 2 mm and 26 ± 1 mm zone of inhibition, respectively. In accordance with CLSI standards, a broth microdilution experiment was conducted to determine the MIC values of the tested substances. The MIC values of clotrimazole and eugenol are 2 µg/ml and 512 µg/ml, respectively. MIC values are presented without measurements of variability because they were consistent in all three replicates.

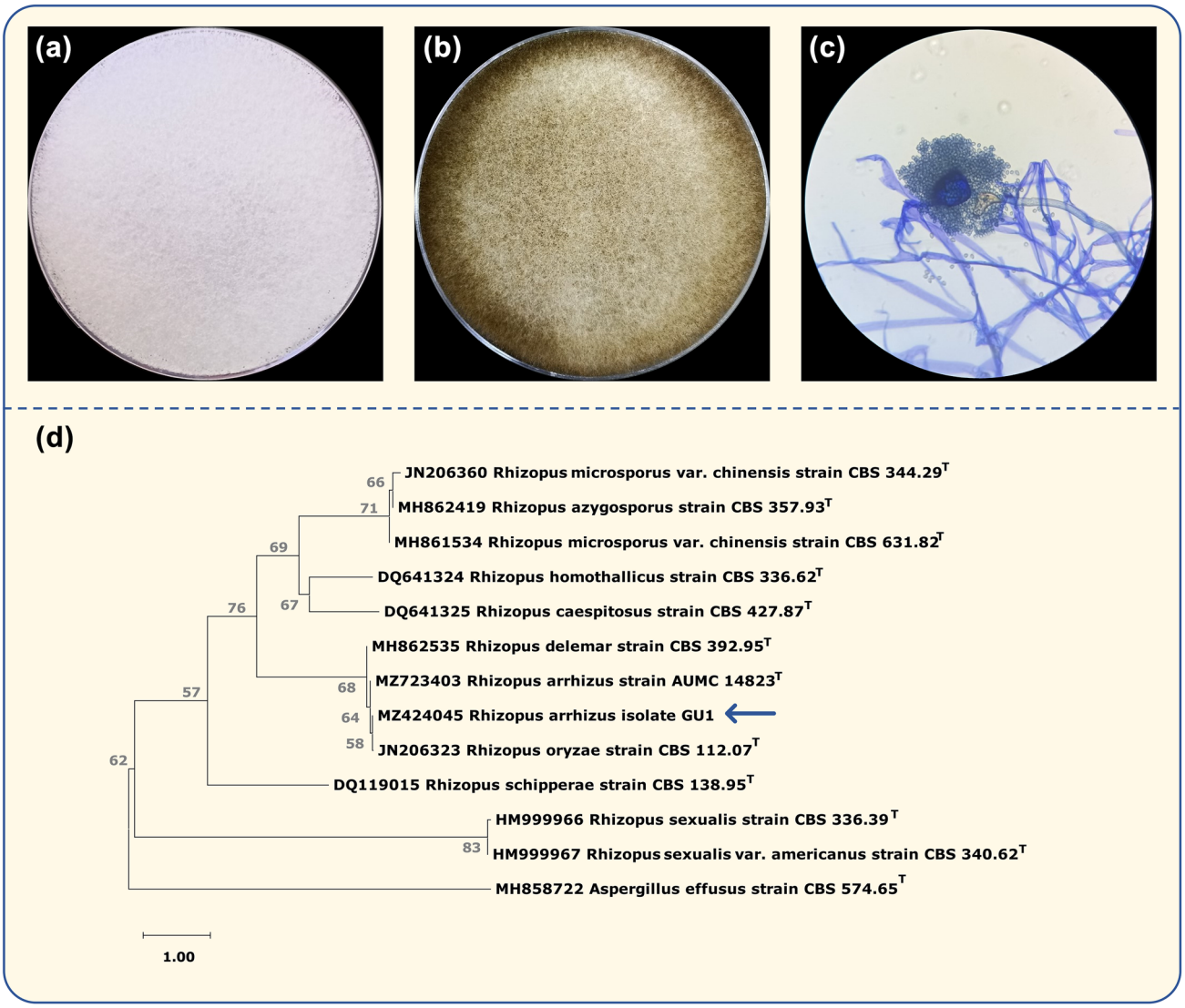


**Fig. 1** Morphological (macro and microscopical), microscopial and molecular examination of mucormycosis causing fungi **a** White, cottony, fluffy, growth with aerial hypha of fungi on PDA plate at 24 h, **b** Dirty white or black hypha of fungi on PDA plate at 96 h and **c** Lactophenol cotton blue stained fungus under 40X magnification **d** Molecular analysis based on ITS sequence compared in the NCBI database using the BLAST library and phylogenetic tree was constructed through neighbor-joining approach using MEGA 11.0 software package. Bootstrap values based on 1000 replications listed as per percentages at the branching points. $^{T}$ represents the type strain

When fungal spores were treated with a variety of eugenol concentrations, ergosterol synthesis was clearly inhibited in a dose-dependent manner. The highest amount of ergosterol production was found in the experimental group that was not given any treatment. On the other hand, experiment group where fungal spores were treated with 256 µg/ml (MIC/2), 170 µg/ml (MIC/3), and 128 µg/ml (MIC/4) by eugenol; $77.11 \pm 3.25\%$, $72.84 \pm 2.5\%$, and $59.76 \pm 2.85\%$ ($p < 0.05$) percent growth inhibition was observed as shown in Fig. 2b**.** In addition, investigation relied on PI-stained cells was carried out to analyse the effectiveness of eugenol on the plasma membrane integrity. As show in Fig. 2c, in comparison to the untreated control, the fungal hyphae exposed to eugenol and clotrimazole for 24 h showed a greater staining intensity due to lower content of ergosterol. The results of fluorescent microscopy indicated that eugenol could impair the integrity of *R. oryzae/R. arrhizus* cell membrane.

## In Silico Analysis of Eugenol with Fungal CYP51B

To confirm our hypothesis, the molecular docking approach was used to understand the interaction between eugenol and fungal protein CYP51B. The Glide module of Schrodinger Maestro was used to dock the test compound eugenol and the positive control clotrimazole with the CYP51B. 2D and 3D interactions of clotrimazole and eugenol with CYP51B

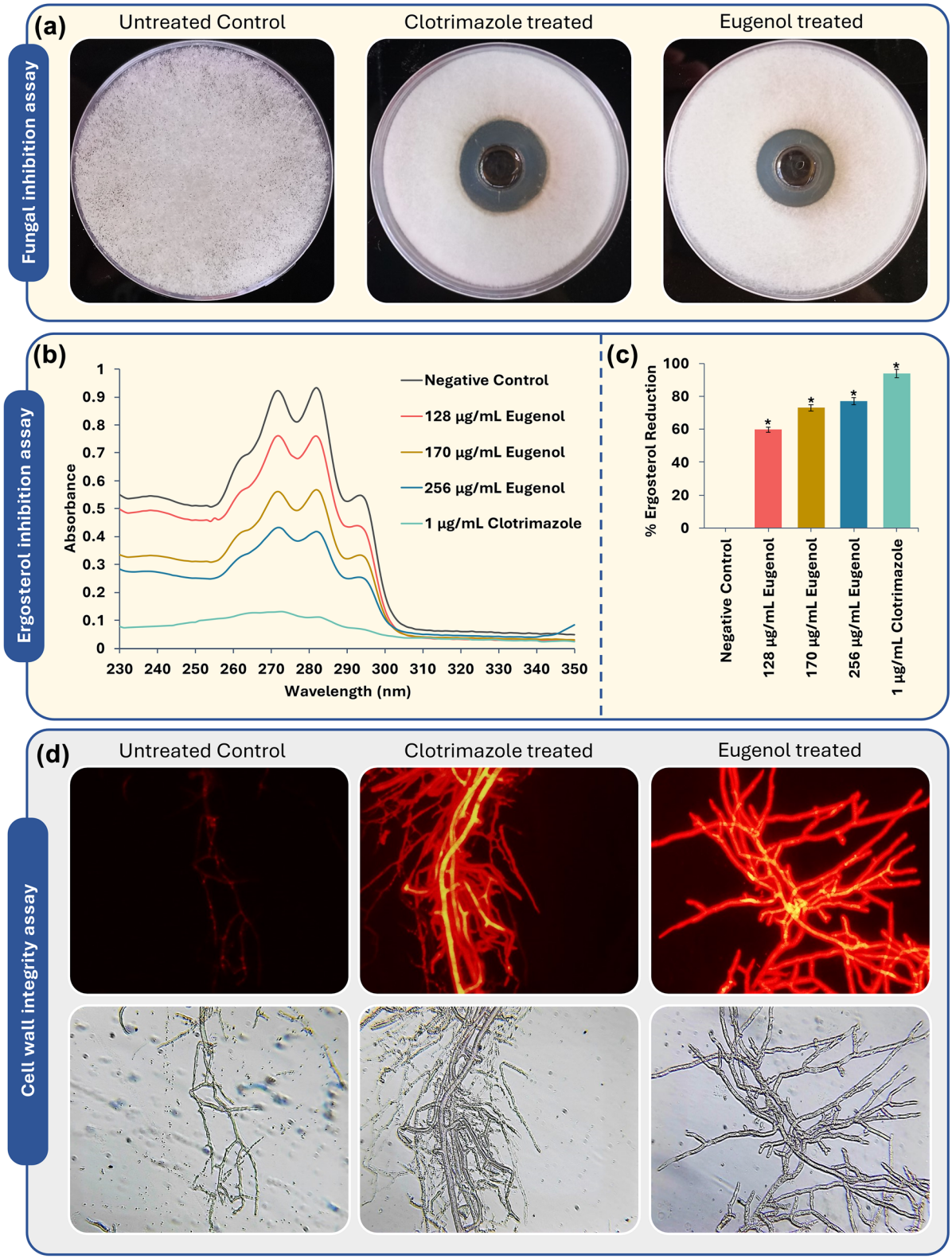


**Fig. 2** In vitro antifungal activity of clotrimazole and eugenol against *R. oryzae/R. arrhizus*. **a** Visual zone of inhibition of *R. oryzae/R. arrhizus* for untreataed control (left), clotrimazole (center), and eugenol (right); **b** UV spectrophotometric sterol analysis graph demonstrating dose-dependent reduction in sterol content; **c** The bar graph illustrating percent decrease in ergosterol content $*p < 0.05$ compared with control; **d** Microscopic observation of hyphae stained with propidium iodide (PI) under fluoroscent microscope (first row) and light microscope (second row) with 40X magnifications shows the

**Table 1** MM-GBSA binding free energy change profiles of Clotrimazole-CYP51B and Eugenol-CYP51B docked complexes

| Ligand | $\Delta G_{Bind}$ (kcal/mol) | $\Delta G_{Coulomb}$ (kcal/mol) | $\Delta G_{Hbond}$ (kcal/mol) | $\Delta G_{Lipo}$ (kcal/mol) | $\Delta G_{Packing}$ (kcal/mol) | $\Delta G_{vdW}$ (kcal/mol) |
|---|---|---|---|---|---|---|
| Clotrimazole | − 47.80 | − 39.55 | − 0.004 | − 41.35 | − 8.21 | − 30.89 |
| Eugenol | − 48.34 | − 32.32 | − 0.67 | − 36.34 | − 0.93 | − 45.66 |

Meaning of abbreviations used in the table are as follows: $\Delta G_{Coulomb}$ coulomb energy, $\Delta G_{Hbond}$ hydrogen-bonding correction, $\Delta G_{Lipo}$ lipophilic energy, $\Delta G_{Packing}$ pi-pi packing correction, $\Delta G_{vdW}$ van der waals energy

are shown in Fig. 2. Clotrimazole interacts with the Tyr113, Phe121, Val126, Thr298, Phe293, Gly294, Cys455, Met494 and heme of CYP51B. This interaction revealed several hydrophobic interactions along with the pi-sulphur and carbon-hydrogen bonds and obtained a docking score of − 7.8 kcal/mol. Furthermore, the $\Delta G_{Bind}$ score obtained from the MM-GBSA free energy analysis was − 47.806 kcal/mol. This negative value indicates that the interaction between the clotrimazole and the protein CYP51B occurs spontaneously. For eugenol, it was observed that it interacts with the CYP51B through making several types of bonds such as pi-alkyl, pi-pi T shaped, carbon hydrogen bond and Van der Waals bonds with Ala290, Val291, Gly294, Thr298, Ile360. As shown in both 2D and 3D representation, eugenol also interacts with the heme present in the CYP51B. The docking score for interaction between eugenol and CYP51B is − 6.6 kcal/mol and free energy evaluation using MM-GBSA yielded a $\Delta G_{Bind}$ score of − 48.34 kcal/mol. In addition to $\Delta G_{Bind}$ energy, calculations for energy, hydrogen-bonding correction, lipophilic energy, pi-pi packing correction and Van der Waals energy is also specified in Table 1 for both the interactions (Fig. 3).

In this investigation, 50 ns MD simulation runs were used to evaluate the Root Mean Square Deviations (RMSD) and interaction strength of CYP51B-clotrimazole and CYP51B-eugenol complexes. Figures 4, 5 represents the protein–ligand RMSD, interaction summary, interaction timeline and histogram of interaction fractions for CYP51B-clotrimazole and CYP51B-eugenol complexes, respectively. For small, globular proteins, RMSD variations in the range of 1 Å to 3 Å are totally reasonable; however, for bigger proteins, the range may expand. However, much larger changes indicate a significant structural shift in protein during MD recordings. In this case, despite of the larger protein, the RMSD value never exceeds 3 Å, indicating that protein stability is satisfactory. The RMSD of the ligand, which is a measure of how stable the ligand is bound at the catalytic site of CYP51B, is shown on the right Y-axis. The value of 'Lig fit Prot' is acceptable in this investigation for both the ligands, because it is not considerably larger than protein RMSD value. As a result of this analysis, it can be determined that clotrimazole and eugenol both interact with CYP51B in a stable manner. Next, the interaction of both the ligands with CYP51B in detail be understood by protein ligand interaction summary image as shown in Figs. 4b, 5b, which shows interaction prevailing between ligand and protein during the MD simulation run, here it is observed that 'Fe' of heme moiety is well recruited by reference drug clotrimazole and test molecule eugenol during the MD simulation run. This interacting 'Fe' further interacts with Cys455, which is the key residue for the inhibition of the protein [25]. This phenomenon is seen at par for both the ligands under study. Further, protein–ligand interaction timeline chart (Figs. 4c, 5c) represents instances when these dynamic bonds are formed and broken with respect to time. Lastly, Protein–Ligand interaction fraction plot for both the complexes show, eugenol to interact with all the amino acids that also interact with clotrimazole (Figs. 4d, 5d). Also, both the ligands interact at par with Cys455 by making ionic bridge. For the plot, interaction fraction represents the value converted from percent interaction, viz. the interaction fraction of 0.4 suggests that 40% of the time of total MD simulation run time (50 ns), the interaction is formed. This value can be 1.0 which in 100% only for the covalent bond, as other interactions (H-bonds, hydrophobic interaction, ionic and water bridges) are dynamic in nature which has a very short life span of around 1 ps, so such bonds keep forming and breaking throughout the MD simulation run and its aggregate value is represented in the chart as interaction fraction.

## Discussion

Fungal infections have increased in frequency over the past few decades and are a major cause of high mortality and morbidity, particularly in immunocompromised people. In recent times, the pandemic of SARS-CoV-2 infection has paved the way for comorbidities associated with secondary infections post COVID-19 [25]. The major fungal culprits belong to the genus of *Rhizopus* (mucormycosis agent), *Aspergillus, Candida, Cryptococcus, Histoplasma,* and *Coccidioides*. All these fungal pathogens are acquiring resistance to routinely used antifungal drugs and therefore scientific community predicts the scenario of human health pertaining to fungal infections to deteriorate in coming time,

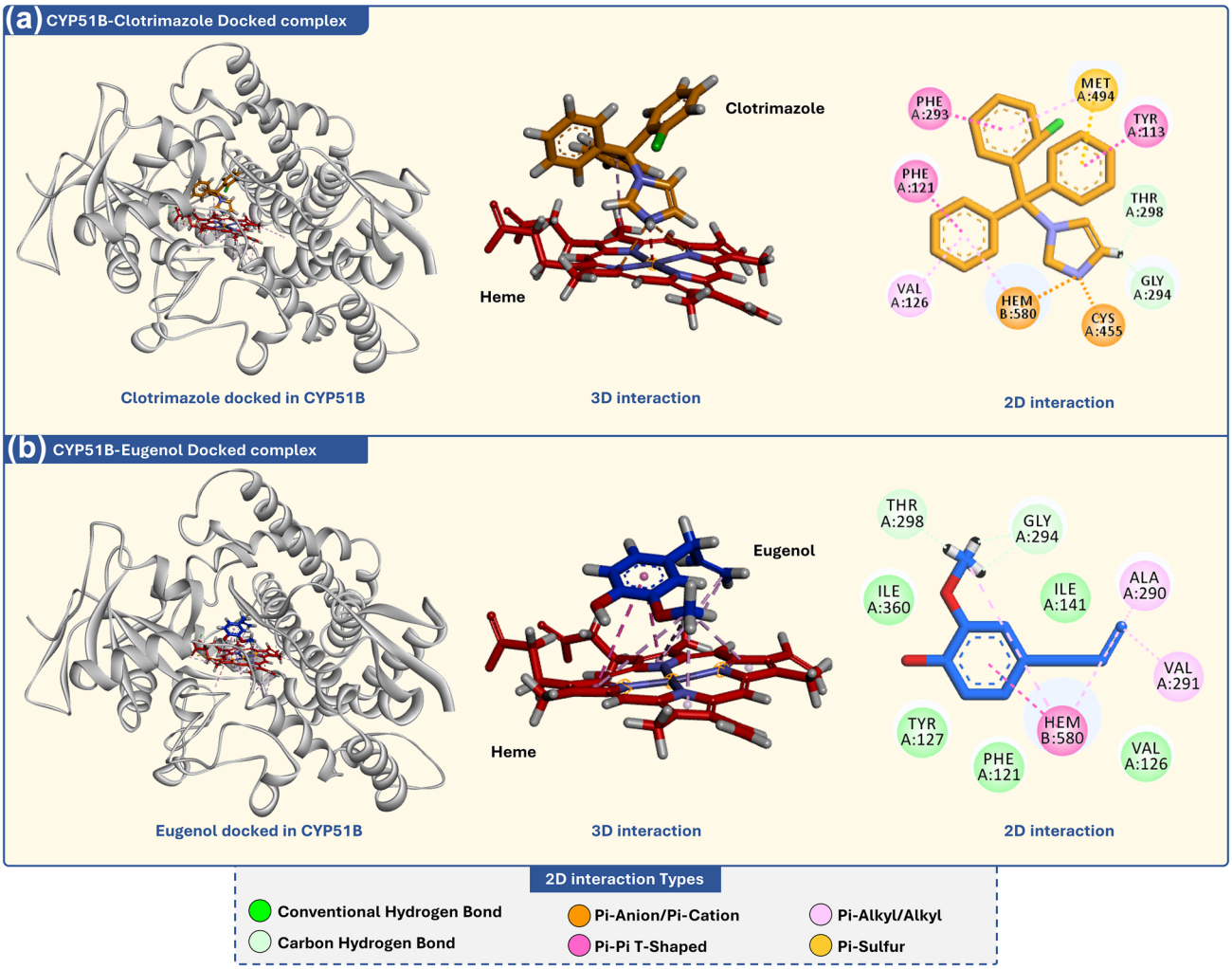


**Fig. 3** Molecular docking of Clotrimazole and Eugenol with CYP51B **a** 3D and 2D interaction profile for clotrimazole with CYP51B, **b** 3D and 2D interaction profile for eugenol with CYP51B

which has elevated the need to identify from nature and or to develop newer antifungal drugs with improved potency of action.

For the research pursued on natural products, there are promising evidence that phytochemicals can inhibit the growth of fungi at exceptionally low concentrations and their MIC are at par with most efficient antifungal drugs, but the limitation is that their mode of action is not accurately studied. Eugenol is one of the natural derivatives of guaiacol which is an aromatic oil with a formula $C_6H_4(OH)(OCH_3)$, where an -allyl chain is added to the aromatic moiety by single portion substitution. Eugenol possessed the antifungal, antibacterial and antiviral potentials [18].

The results of our in vitro antifungal assays show the potential antifungal activity of eugenol against clinically isolated *R. oryzae/R. arrhizus* (mucormycosis agent). Previous investigations [35–37] have shown that eugenol and eugenol-containing essential oils have antifungal action against yeast and filamentous fungus species. In accordance with the literature, our experiments demonstrated that eugenol has antifungal activity at microgram level. The primary molecular targets for antifungal agents are various such as enzymes and other molecules involved in cell wall synthesis, plasma membrane synthesis, fungal DNA and protein synthesis, cellular function-related, and virulence factors [38]. In light of the fact that the majority of antifungal medicines impede the manufacture of ergosterol, a crucial component of fungal cell membrane [6], the impact of eugenol on ergosterol biosynthesis in *R. oryzae/R. arrhizus* was investigated. We hypothesise that the antifungal effect of eugenol is related to the inhibition of the Lanosterol 14-α-Demethylase enzyme, based on the findings of the given investigation and prior information that the antifungal azole medications block ergosterol production by inhibiting a key enzyme, Lanosterol 14-α-Demethylase (CYP51) [39], (CYP51B, in *R. oryzae/R. arrhizus*).

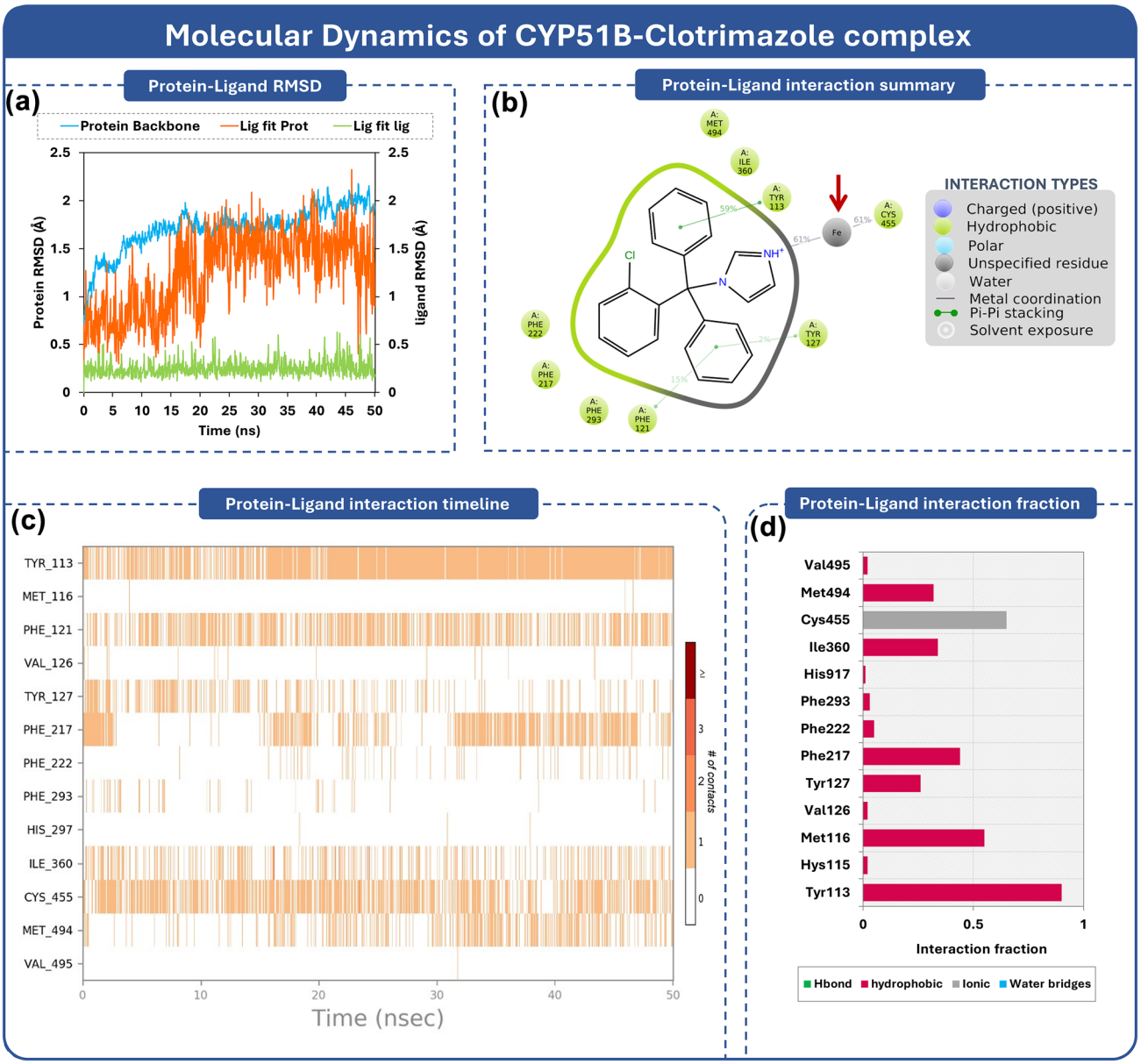


**Fig. 4** MD simulations of CYP51B-Clotrimazole docked complex for 50 ns **a** RMSD profile, **b** Ligand interaction diagram showing percent of total time a particular interaction is involved, **c** Timeline representation of the interactions of ligand with amino acids present in binding site of CYP51B **d** Interaction fraction of crucial interacting amino acids of CYP51B with clotrimazole

In current study, in silico analysis was performed to assess the interaction of eugenol with CYP51B of *R. oryzae/R. arrhizus*. Molecular docking was one of them which simply predicts the type of interaction that may occur between a protein and a ligand for a certain pose, but it does not predict the strength of the interaction [40], and hence MD simulation was also performed to validate the interaction of eugenol with fungal CYP51B. MD simulations aid in overcoming this limitation of molecular docking. MD simulations are performed to determine if the assurance provided by the docking assessment for a ligand–protein interaction will really translate into practical terms [41, 42]. Such MD simulation study can well establish the interaction of ligands with protein receptors with great degree of fidelity and scientific fraternity with increasing computational power make use of it to validate the hypothesis [43–45]. The current manuscript demonstrates the interaction of eugenol with CYP51B for making use of MD simulations which by far, to the best of our knowledge is not done making this the first report to assess the efficacy of eugenol to interact with CYP51B, where the interaction is found to be promising and at par with reference azole drug, clotrimazole.

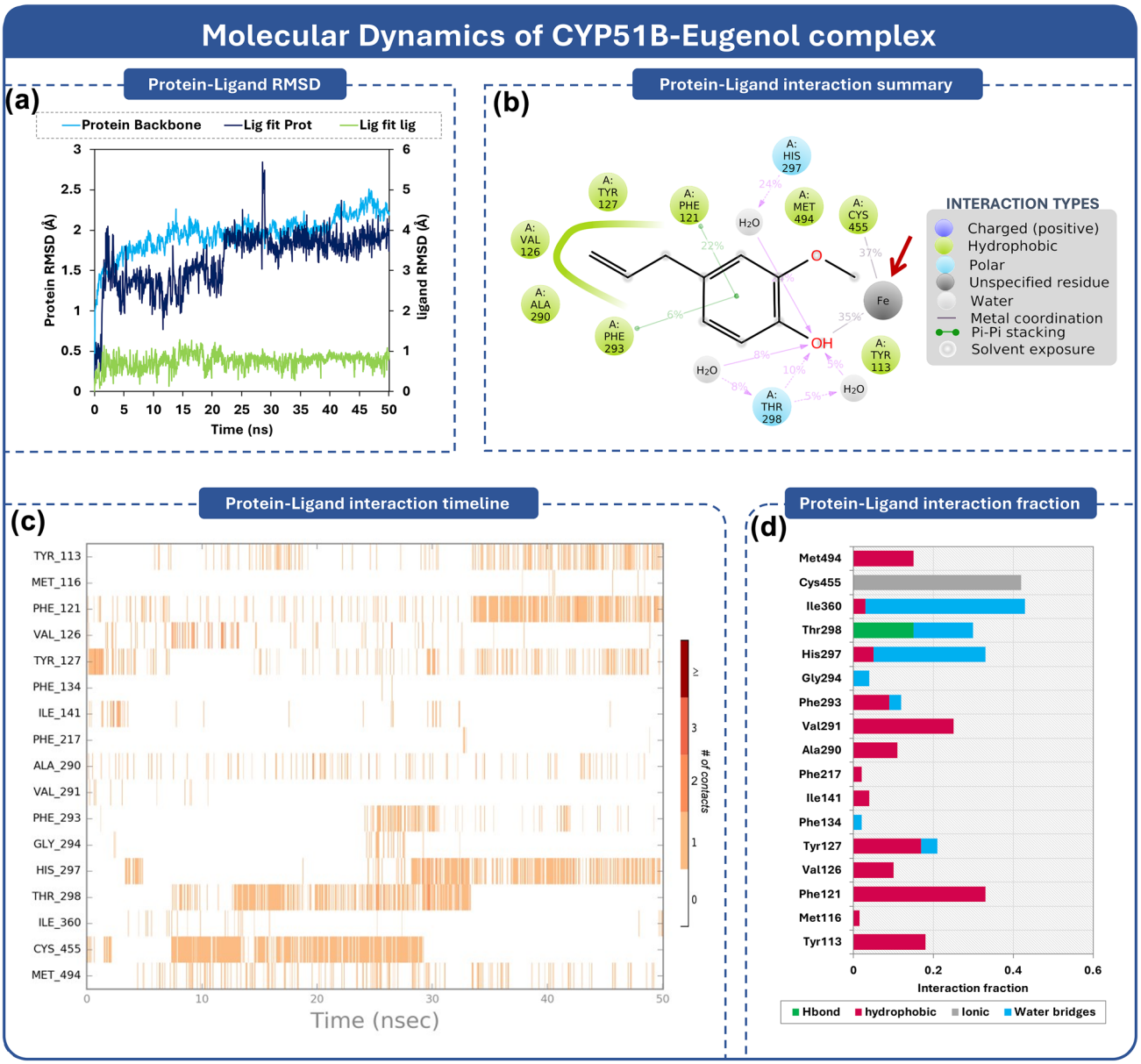


**Fig. 5** MD simulations of CYP51B-Eugenol docked complex for 50 ns **a** RMSD profile, **b** Ligand interaction diagram showing percent of total time a particular interaction is involved, **c** Timeline representation of the interactions of ligand with amino acids present in binding site of CYP51B **d** Interaction fraction of crucial interacting amino acids of CYP51B with eugenol

## Conclusion

In present investigation, eugenol was found to have antifungal potential towards mucormycosis agent *R. oryzae/R. arrhizus*, with a MIC value in the microgram range. In addition, as the amount of eugenol increased, the amount of ergosterol in the fungus reduced, suggesting that it inhibits the ergosterol biosynthesis pathway. In silico analysis of eugenol with CYP51B, a key enzyme in the ergosterol pathway, strengthens the in vitro findings. Consequently, eugenol exhibited potential antifungal activity against *R. oryzae/R. arrhizus*, suggesting that it might be used in the development of targeted medicines to combat CYP51-mediated azole resistance.

**Acknowledgements** All authors are thankful to Dr. Bhavin Kapadiya of Speciality Microtech Lab, Ahmedabad, Gujarat, India for providing left over tissue sample. Authors acknowledge DST-FIST Sponsored Department of Microbiology and Biotechnology, School of Sciences, Gujarat University, for providing necessary facilities to perform experiments and GSBTM (DST, Government of Gujarat) for providing Bioinformatics Node facility.

**Author Contributions** J.P. and D.G. wrote the manuscript, J.P., L.P., and P.R. performed experiments, prepared figures, and tables, J.P., R.M.R. and D.G. conceptualized the idea, S.K.P., D.A. and D.G. critically proofread the manuscript. All authors have seen and approved the manuscript.

**Funding** This work was supported by Gujarat State Biotechnology Mission (GSBTM) under Network program on Antimicrobial Resistance, Superbugs, and One Health: Human Health Care Node [GSBTM/JD(R&D)/616/21–22/1236] and Research Support Scheme (RSS) of GSBTM [GSBTM/JD(R&D)/610/20–21/365–371]. JP is grateful for support of the University Grants Commission (UGC), New Delhi, India for providing fellowship for the award of 'CSIR-NET Junior Research Fellowship (JRF)'.

**Data Availability** All the relevant data is contained within the manuscript. Additional raw data will be available upon request.

**Code Availability** Not applicable.

## Declarations

**Conflict of interest** The authors have no competing interests to declare that are relevant to the content of this article.

**Ethical Approval** This article does not contain any studies with human participants or animals performed by any of the authors.

**Informed Consent** Not applicable.

**Consent for Publication** Not applicable.

## References

1. Baldin C, Ibrahim AS (2017) Molecular mechanisms of mucormycosis—The bitter and the sweet. PLoS Pathog. https://doi.org/10.1371/journal.ppat.1006408
2. Ibrahim AS, Spellberg B, Walsh TJ, Kontoyiannis DP (2012) Pathogenesis of mucormycosis. Clin Infect Dis 54:S16. https://doi.org/10.1093/cid/cir865
3. Ahmed N, Mahmood MS, Ullah MA et al (2022) COVID-19-associated Candidiasis: possible patho-mechanism, predisposing factors, and prevention strategies. Curr Microbiol 79:127. https://doi.org/10.1007/s00284-022-02824-6
4. Soliman SSM, Baldin C, Gu Y et al (2021) Mucoricin is a ricin-like toxin that is critical for the pathogenesis of mucormycosis. Nat Microbiol 6:313–326. https://doi.org/10.1038/s41564-020-00837-0
5. Masood MM, Irfan M, Khan P et al (2018) 1,2,3-Triazole-quinazolin-4(3H)-one conjugates: evolution of ergosterol inhibitor as anticandidal agent. RSC Adv 8:39611–39625. https://doi.org/10.1039/c8ra08426b
6. Ahmad A, Khan A, Manzoor N, Khan LA (2010) Evolution of ergosterol biosynthesis inhibitors as fungicidal against Candida. Microb Pathog 48:35–41. https://doi.org/10.1016/j.micpath.2009.10.001
7. Nagy G, Kiss S, Varghese R et al (2021) Characterization of three pleiotropic drug resistance transporter genes and their participation in the azole resistance of *Mucor circinelloides*. Front Cell Infect Microbiol 11:1–15. https://doi.org/10.3389/fcimb.2021.660347
8. Shafiei M, Peyton L, Hashemzadeh M, Foroumadi A (2020) History of the development of antifungal azoles: a review on structures, SAR, and mechanism of action. Bioorg Chem 104:104240. https://doi.org/10.1016/J.BIOORG.2020.104240
9. Ganeshkumar A, Suvaithenamudhan S, Rajaram R (2021) In vitro and in silico analysis of ascorbic acid towards lanosterol 14-α-demethylase enzyme of fluconazole-resistant *Candida albicans*. Curr Microbiol 78:292–302. https://doi.org/10.1007/S00284-020-02269-9/TABLES/2
10. Prajapati J, Goswami D, Rawal RM (2021) Endophytic fungi: a treasure trove of novel anticancer compounds. Curr Res Pharmacol Drug Discov 2:100050. https://doi.org/10.1016/j.crphar.2021.100050
11. Almeida CF, Teixeira N, Oliveira A et al (2021) Discovery of a multi-target compound for estrogen receptor-positive (ER+) breast cancer: involvement of aromatase and ERs. Biochimie 181:65–76. https://doi.org/10.1016/J.BIOCHI.2020.11.023
12. Pantaleão SQ, Philot EA, de Paula H et al (2022) Virtual screening and in vitro assays of novel hits as promising DPP-4 inhibitors. Biochimie 194:43–50. https://doi.org/10.1016/J.BIOCHI.2021.12.007
13. Abraham P, George S, Kumar KS (2014) Novel antibacterial peptides from the skin secretion of the Indian bicoloured frog *Clinotarsus curtipes*. Biochimie 97:144–151. https://doi.org/10.1016/J.BIOCHI.2013.10.005
14. Choi H, Lee DG (2014) Antifungal activity and pore-forming mechanism of astacidin 1 against *Candida albicans*. Biochimie 105:58–63. https://doi.org/10.1016/J.BIOCHI.2014.06.014
15. Priha O, Virkajärvi V, Juvonen R et al (2014) Quorum sensing signalling and biofilm formation of brewery-derived bacteria, and inhibition of signalling by natural compounds. Curr Microbiol 69:617–627. https://doi.org/10.1007/S00284-014-0627-3/FULLTEXT.HTML
16. Khan SN, Khan S, Misba L et al (2019) Synergistic fungicidal activity with low doses of eugenol and amphotericin B against *Candida albicans*. Biochem Biophys Res Commun 518:459–464. https://doi.org/10.1016/j.bbrc.2019.08.053
17. Mohammadi Nejad S, Özgüneş H, Başaran N (2017) Pharmacological and toxicological properties of eugenol. Turkish J Pharm Sci 14:201–206. https://doi.org/10.4274/tjps.62207
18. Ulanowska M, Olas B (2021) Biological properties and prospects for the application of eugenol—a review. Int J Mol Sci. https://doi.org/10.3390/ijms22073671
19. Nunes DOS, Vinturelle R, Martins FJ et al (2021) Biotechnological potential of eugenol and thymol derivatives against *Staphylococcus aureus* from Bovine Mastitis. Curr Microbiol 78:1846–1855. https://doi.org/10.1007/S00284-021-02344-9/FULLTEXT.HTML
20. Zhang YJ, Zhang S, Liu XZ et al (2010) A simple method of genomic DNA extraction suitable for analysis of bulk fungal strains. Lett Appl Microbiol 51:114–118. https://doi.org/10.1111/J.1472-765X.2010.02867.X
21. Tamura K, Stecher G, Kumar S (2021) MEGA11: molecular evolutionary genetics analysis version 11. Mol Biol Evol 38:3022–3027. https://doi.org/10.1093/molbev/msab120
22. Devillers J, Steiman R, Seigle-Murandi F (1989) The usefulness of the agar-well diffusion method for assessing chemical toxicity to bacteria and fungi. Chemosphere 19:1693–1700. https://doi.org/10.1016/0045-6535(89)90512-2
23. Zhou D, Wang Z, Li M et al (2018) Carvacrol and eugenol effectively inhibit *Rhizopus stolonifer* and control postharvest soft rot decay in peaches. J Appl Microbiol 124:166–178. https://doi.org/10.1111/jam.13612
24. Shaw WHC, Jefferies JP (1953) The determination of ergosterol in yeast. Part I. the ultra-violet absorption of purified ergosterol. Analyst 78:509b–5514. https://doi.org/10.1039/AN953780509B
25. Prajapati J, Rao P, Poojara L et al (2021) Unravelling the antifungal mode of action of curcumin by potential inhibition of CYP51B: a computational study validated in vitro on mucormycosis agent *Rhizopus oryzae*. Arch Biochem Biophys 712:109048. https://doi.org/10.1016/j.abb.2021.109048
26. Sastry GM, Adzhigirey M, Sherman W (2013) Protein and ligand preparation: parameters, protocols, and influence on virtual screening enrichments. J Comput Aided Mol Des 27:221–234. https://doi.org/10.1007/s10822-013-9644-8
27. Halgren TA, Murphy RB, Friesner RA et al (2004) Glide: a new approach for rapid, accurate docking and scoring. 2. Enrichment

factors in database screening. J Med Chem 47:1750–1759. https://doi.org/10.1021/jm030644s
28. Shukla A, Parmar P, Rao P et al (2020) Twin peaks: presenting the antagonistic molecular interplay of curcumin with LasR and LuxR quorum sensing pathways. Curr Microbiol. https://doi.org/10.1007/s00284-020-01997-2
29. Wang W, Donini O, Reyes CM, Kollman PA (2001) Biomolecular simulations: recent developments in force fields, simulations of enzyme catalysis, protein-ligand, protein-protein, and protein-nucleic acid noncovalent interactions. Annu Rev Biophys Biomol Struct 30:211–243
30. Wang J, Hou T, Xu X (2006) Recent advances in free energy calculations with a combination of molecular mechanics and continuum models. Curr Comput Aided-Drug Des 2:287–306. https://doi.org/10.2174/157340906778226454
31. Kollman PA, Massova I, Reyes C et al (2000) Calculating structures and free energies of complex molecules: Combining molecular mechanics and continuum models. Acc Chem Res 33:889–897. https://doi.org/10.1021/ar000033j
32. Massova I, Kollman PA (2000) Combined molecular mechanical and continuum solvent approach (MM- PBSA/GBSA) to predict ligand binding. Perspect Drug Discov Des 18:113–135. https://doi.org/10.1023/A:1008763014207
33. Bowers KJ, Chow E, Xu H, et al (2006) Scalable algorithms for molecular dynamics simulations on commodity clusters. In: Proceedings of the 2006 ACM/IEEE Conference on Supercomputing, SC'06. ACM Press, New York p 84
34. Dolatabadi S, de Hoog GS, Meis JF, Walther G (2014) Species boundaries and nomenclature of *Rhizopus arrhizus* (syn. *R. oryzae*). Mycoses 57:108–127. https://doi.org/10.1111/MYC.12228
35. Azeredo CMO, Santos TG, de Maia BHL, Soares MJ (2014) In vitro biological evaluation of eight different essential oils against *Trypanosoma cruzi*, with emphasis on *Cinnamomum verum* essential oil. BMC Complement Altern Med 14:1–8. https://doi.org/10.1186/1472-6882-14-309
36. Sharma A, Rajendran S, Srivastava A et al (2017) Antifungal activities of selected essential oils against *Fusarium oxysporum* f. sp. lycopersici 1322, with emphasis on Syzygium aromaticum essential oil. J Biosci Bioeng 123:308–313. https://doi.org/10.1016/j.jbiosc.2016.09.011
37. De Oliveira PF, Mendes JM, De Oliveira LE (2013) Investigation on mechanism of antifungal activity of eugenol against *Trichophyton rubrum*. Med Mycol 51:507–513. https://doi.org/10.3109/13693786.2012.742966
38. Perfect JR (2017) The antifungal pipeline: a reality check. Nat Rev Drug Discov 16:603–616. https://doi.org/10.1038/nrd.2017.46
39. Becher R, Wirsel SGR (2012) Fungal cytochrome P450 sterol 14α-demethylase (CYP51) and azole resistance in plant and human pathogens. Appl Microbiol Biotechnol 95:825–840. https://doi.org/10.1007/s00253-012-4195-9
40. Goswami D (2021) Comparative assessment of RNA-dependent RNA polymerase (RdRp) inhibitors under clinical trials to control SARS-CoV2 using rigorous computational workflow. RSC Adv 11:29015–29028. https://doi.org/10.1039/d1ra04460e
41. Rao P, Goswami D, Rawal RM (2021) Revealing the molecular interplay of curcumin as *Culex pipiens* Acetylcholine esterase 1 (AChE1) inhibitor. Sci Rep 11:1–18. https://doi.org/10.1038/s41598-021-96963-8
42. Prajapati J, Patel R, Goswami D et al (2021) Sterenin M as a potential inhibitor of SARS-CoV-2 main protease identified from MeFSAT database using molecular docking, molecular dynamics simulation and binding free energy calculation. Comput Biol Med 135:104568. https://doi.org/10.1016/j.compbiomed.2021.104568
43. Shukla A, Shukla G, Parmar P et al (2021) Exemplifying the next generation of antibiotic susceptibility intensifiers of phytochemicals by LasR-mediated quorum sensing inhibition. Sci Rep 11:1–23. https://doi.org/10.1038/s41598-021-01845-8
44. Parmar P, Rao P, Sharma A et al (2021) Meticulous assessment of natural compounds from NPASS database for identifying analogue of GRL0617, the only known inhibitor for SARS-CoV2 papain-like protease (PLpro) using rigorous computational workflow. Mol Divers. https://doi.org/10.1007/s11030-021-10233-3
45. Patel R, Prajapati J, Rao P et al (2021) Repurposing the antibacterial drugs for inhibition of SARS-CoV2-PLpro using molecular docking, MD simulation and binding energy calculation. Mol Divers. https://doi.org/10.1007/s11030-021-10325-0